Exome Sequencing Reveals a Heterozygous OAS3 Mutation in a Chinese Family With Juvenile-Onset Open-Angle Glaucoma

Xiaoqiang Xiao,[1] Chukai Huang,[1] Yingjie Cao,[1] Shaowan Chen,[1] Yanxuan Xu,[1] Haoyu Chen,[1] Chipui Pang,[1,2] and Mingzhi Zhang[1]

[1]Joint Shantou International Eye Center, Shantou University and the Chinese University of Hong Kong, Shantou, China
[2]Department of Ophthalmology and Visual Sciences, the Chinese University of Hong Kong, Hong Kong, China

Correspondence: Xiaoqiang Xiao, Shantou Eye Center, Dongxia Road North, Jinpin District, Shantou, Guangdong Province, China; lijingyu19801980@163.com
Mingzhi Zhang, Shantou Eye Center, Dongxia Road North, Jinpin district, Shantou, Guangdong Province, China; zmz@jsiec.org.

XX and CH contributed equally to the work presented here and should therefore be regarded as equivalent authors.

Submitted: May 17, 2019
Accepted: August 16, 2019

Citation: Xiao X, Huang C, Cao Y, et al. Exome sequencing reveals a heterozygous OAS3 mutation in a Chinese family with juvenile-onset open-angle glaucoma. *Invest Ophthalmol Vis Sci*. 2019;60:4277–4284. https://doi.org/10.1167/iovs.19-27545

Purpose. Juvenile-onset open-angle glaucoma (JOAG), if left untreated, will lead to severe visual disability. The purpose of this study was to identify the disease-causing mutations in a Chinese JOAG family.

Methods. We recruited a Chinese JOAG family and unrelated primary open-angle glaucoma (POAG) patients (270, Chinese), and performed whole-exome sequencing (WES) to screen the sequence variations. Variants identified by WES were validated by Sanger sequencing. Subsequently, qPCR and Western blotting were used to determine the expression of wild-type (WT) and its mutated-type (MT) of 2′-5′-oligoadenylate synthetase 3 (*OAS3*) genes.

Results. Seventeen heterozygous candidate variants were revealed in the JOAG family based on the screening of WES data. Of those, the heterozygous variant exon11:c.2299C>T: p.Arg767Cys in *OAS3*, a gene used to synthesize 2′-5′-oligoadenylate (2–5A), co-segregates with the disease phenotype. One unrelated POAG patient also carried this variant, but this variant was absent in 200 nonglaucoma healthy controls. Analysis of the Arg767Cys mutation with PolyPhen2, CADD, and SIFT all suggest that it is pathogenic. This arginine residue is highly conserved in all selected OAS3 orthologs. On the other hand, in peripheral blood samples, the mRNA expression of OAS3 in patients significantly decreased compared with unaffected controls. Moreover, the expression level of recombinant OAS3 protein (mutated Arg767Cys) also observably reduced compared with level of WT protein in HEK293T cells.

Conclusions. Our study revealed a heterozygous mutation in *OAS3* from a Chinese JOAG family. And this mutation showed a deleterious effect to the expression of OAS3.

Keywords: JOAG, OAS3, WES, glaucoma

Glaucoma is a heritable eye disease, which is defined as an acquired loss of retinal ganglion cells and axons within the optic nerve or optic neuropathy, leading to irreversible visual field loss and eventually to blindness.[1,2] Primary open-angle glaucoma (POAG) is the most common form of glaucoma, which consists of juvenile-onset (JOAG) and adult-onset open-angle glaucoma based on the onset age of disease.[1,2] Characterizing the genetic factors influencing an individual's susceptibility to POAG is an important step toward understanding its etiology. Previous study showed that the range of additive inheritance for POAG was 24% to 42%.[3] Currently, many disease-causing variants were distributed to several genes including *MYOC*, *OPTN*, *CYP1B1*, *NTF4*, *TBK1*, and *WDR36* in glaucoma.[4,5] Also, the genome-wide association studies revealed *CAV1*/CAV2, *TMCO1, SIX6, CDKN2B-AS1, FNDC3B, ANKRD55-MAP3K1, FMNL2, LMX1B, LHPP, HMGA2, NR1H3, PDE7BTMTC2, IKZF2, MEIS2, CADM2, DGKG, ANKH, RAMP, MADD, SEPT9, EXOC2, LOXL1, ABCA1, ARHGEF12, AFAP1*, and *GMDS* as potential POAG-causing genes.[4–10] However, those discovered loci explain only a small proportion of genetic contribution to POAG risk, and only a few have been investigated in functional studies (e.g., *MYOC*, *SIX6*, *FMNL2, LMX1B*, and *CAV1/2*).[10] Therefore, identifying more disease-causing mutations especially for JOAG patients are important for diagnosis and treatment of glaucoma.

Whole-exome sequencing (WES) is widely used strategy for detection of protein coding and splicing variants associated with inherited diseases.[11,12] The present work was to identify disease-causing mutations in a Chinese JOAG family using WES.

Materials and Methods

Clinic Evaluation and Blood Samples Acquirement

POAG family members, sporadic POAG patients, and nonglaucoma healthy controls at the Shantou University/Chinese University of Hong Kong Joint Shantou International Eye Center, Shantou, Guangdong Province, China, were recruited into this study. Written informed consents were obtained from the participants or their guardians. The ethic committee of Joint Shantou International Eye Center approved this study, which strictly follows the tenets of the Declaration of Helsinki. All patients in this family showed high IOP and their onset ages were younger than or close to 40 years old (Table 1). Patient (II:3) in the family has already become blind. In the 270 recruited sporadic glaucoma patients, 55 patients were JOAG

Table 1. Clinical Features of the Analyzed Family

Collection Date (y/mo/d)	Pedigree Code No.	DOB	Sex/Age/ Diagnosis Age	BCVA, OD/OS	VF (MD), OD/OS	Vertical/Horizontal Cup/ Disc Ratio (OD/OS)	Highest IOP	
							OD	OS
2008/2/14	III:12	1973/10/15	M/35/35	1.2/1.5	−6.38/−3.88	(0.7/0.6)/(0.7/0.6)	35	27
2008/2/14	III:14	**1977/10/3**	M/31/31	0.3/0.4 −1.5D=1.2	−18.27/−1.87	(0.45/0.45)/(0.3/0.3)	39	30
2008/2/14	III:10	1970/10/9	M/38/38	0.5/0.4 −2*75=1 −2*105=1	0.21/−0.85	(0.45/0.4)/(0.35/0.35)	33	32
2008/3/6	II:3	1931/3/1	M/77/40	NLP NLP	NA	1.0/1.0	45.3	15.6
2018/5/25	IV:2	1993/2/2	F/26	NA	−2.82/−1.74	(0.3/0.2)/(0.4–0.3)	14.6	13.7
2018/5/25	IV:3	1995/1/1	M/24	NA	−3.28/−2.10	(0.2/0.2)/(0.2/0.2)	14	14
2008/5/25	IV:4	2000/2/15	F/8	NA	−2.69/−2.50	(0.4/0.4)/(0.4/0.4)	18	15
2018/5/25	IV:5	2004.02.10	F/15	NA	NA	(0.35/0.35)/(0.35/0.35)	11	15
2008/5/25	IV:6	2004/4/24	M/4	NA	NA	(0.3/0.3)/(0.3/0.3)	13	12
2008/5/25	IV:7	2003/3/30	F/5	NA	NA	(0.3/0.3)/(0.3/0.3)	17	17
2008/6/10	III:11	1972	F/36	NA	NA	0.3/0.3	14.4	15.4
2008/6/10	III:13	1973	F/35	NA	NA	(0.1/0.1)/(0.1/0.1)	14.2	16
2008/6/10	III:15	1978	F/30	NA	−1.60/−2.69	(0.4/0.3)/(0.4/0.3)	13.8	14.1
2018/6/10	IV:8	2007	F/11	NA	NA	(0.3/0.3)/(0.3/0.3)	13.5	12.7
2009/3/2	III:1	1951/10/23	M/59	NA	−2.98/−2.48	(0.3/0.2)/(0.3/0.2)	14.5	12.7
2009/3/2	II:2	1927	F/82	NA	NA	NA	11.2	14.4
2009/3/2	III:7	1963	F/46	NA	NA	NA	15.3	14.5
2009/3/2	III:3	1955	M/54	NA	NA	0.3/0.3	14.9	13.2
2009/3/2	III:2	1953	F/56	NA	NA	NA	11.4	14.2
2009/3/2	III:4	1958/3/23	M/52	NA	−4.37/−3.47	(0.7/0.6)/(0.6/0.5)	14.9	14.6
2009/3/2	III:8	1969/12/20	M/41	NA	−2.13/−1.91	(0.5/0.4)/(0.5/0.4)	10.1	11.5

The value in bold indicates that the screened OAS3 variant present in patients, but not in healthy controls. BCVA, best-corrected visual acuity; DOB, date of birth; VF (MD), visual field mean defect.

with high IOP, 49 patients with normal-tension glaucoma, and others non-JOAG with high IOP. The definition of JOAG is based on the onset age between 3 and 40 years old, and an IOP elevated greater than 22 mm Hg is considered as high IOP. Patients showed characteristic optic disc damage and/or visual field damage, and open angles under gonioscopy. The non-glaucoma control subjects with their age older than 60 years were free from ophthalmic or systemic diseases except for some mild cataract.

WES and Candidate Mutations Screening

Peripheral blood samples obtained from the patients and controls were used for the total genomic DNA extraction with QIAamp DNA Blood Mini Kit (QIANEN, Beijing, China). Then, a Nanodrop1000 Spectrophotometer was selected to quantify the DNA samples. Four patients, one healthy control within the family, as well as 55 sporadic JOAG patients were sent for WES using the extracted genomic DNAs via a commercially available service provided by ANOROAD (Beijing, China). Briefly, the whole exomes were captured using Agilent Sure Select All Human Exon v5.0 kit (Agilent Technologies, Santa Clara, CA, USA). Then, the HiSeq 2500PE100 (Illumina, San Diego, CA, USA) platform was selected for paired-end sequencing with read lengths of 100 bp and average coverage depth of at least 100-fold for each sample. The raw data from the sequencing were mapped to the UCSC hg19 via Burrows-Wheeler Alignment (BWA) tool, then using the SAMtools (http://www.htslib.org/, in the public domain) to detect the single nucleotide polymorphisms and insertion/deletions. To obtain the candidate variants, we first excluded high-frequency variants (minor allele frequency >0.05) in the 1000 Genome project (ftp://ftp.1000genomes.ebi.ac.uk/vol1/ftp/, in the public domain) and Exome Aggregation Consortium (ExAC) (http://exac.broadinstitute.org/, in the public domain), and then excluded intergenic variants, intronic variants, and synonymous mutations. All the reported genes were also excluded following the above filtered steps. Furthermore, we used the protein structure prediction programs Polyphen-2 (http://genetics.bwh.harvard.edu/pph2/index.shtml), Sorting Intolerant From Tolerant (SIFT) (http://sift.jcvi.org), Mutation Taster (http://www.mutationtaster.org/), and CADD to evaluate the effect of mutation to the function and structure of proteins.

PCR-based Sanger Sequencing Analysis

After the mutation screening, we performed PCR with the designated primer sets in Table 2 and used Sanger sequencing to confirm the candidate variants within the family's members. The results of Sanger sequence were also used for the cosegregation analysis. We further performed PCR-Sanger sequence to test the disease-causing variants in sporadic glaucoma patients and 200 nonglaucoma controls.

Gene Expression of OAS3 Analysis

Images of in situ hybridization for OAS3 transcriptional expression in mouse embryonic tissues were extracted from GenePaint (http://www.genepaint.org, in the public domain). Fresh blood samples of patients carrying the OAS3 mutation or healthy controls were used for total RNA extraction with TRIZol reagent (Invitrogen, Carlsbad, CA, USA). The first strand cDNA was then synthesized with 2 μg above total RNA as the template using SuperScript IV VILO Master Mix kit (Thermo Scientific, Waltham, MA, USA). Quantitative PCR (qPCR) analysis was performed with the 7500 Real-Time PCR System (ABI) using SYBR Green Premix Ex Taq II (Takara, Dalian,

Table 2. Primer Set Used to Confirm Candidate Variants

Primer Name	Sequence (5′–3′)	Usage
KIF26A_4F	CTCTGCCAGCCCTGATTTCT	Mutation confirmation
KIF26A_4R	CCATCCACTCGTCTCAGCA	
RIPK3_10F	AACTGCCTTGCCCACATG	Mutation confirmation
RIPK3_10R	GTCAGTTTGTGGGCAGGC	
MRPL9_3F	GGACGACAACTCCCTCTATACA	Mutation confirmation
MRPL9_3R	TTGGACATTGGCTGGGCTT	
KLRD1_F	TAGTAGCCCCTGAAGTGTGG	Mutations confirmation
KLRD1_R	TGAGCTGAAATTGCACCAGT	
KIDINS220_F	GACTCCCTGAAACTGTCCCT	Mutation confirmation
KIDINS220_R	ATGACCGTGTGAAGGACCAA	
SMARCC2_F	TCACACCCATAGTCCAAGCT	Mutation confirmation
SMARCC2_R	AGGTGATCTGATTCTAGGAGACA	
ACIN1_6F	ATTCATCCTCTAGCCGGTCC	Mutation confirmation
ACIN1_6R	GTGAAGGAGAGTAAAGGAGGCT	
OAS3_11F	CCTCAGAACCTACCCACCAG	Mutation confirmation
OAS3_11R	TCCTCCCATGACCACTTTCC	
SHMT2_4F	AGTGTCAGGGATGGTGCTC	Mutation confirmation
SHMT2_4R	CCTCATCCACTGTGACATGC	
OR6C75_F	ACCCTCACCCTTTCAGATCC	Mutation confirmation
OR6C75_R	GGAGGCACAGAAATCCAACT	
E2F6–6F	CGGCAGAAGTTAAAAGTCCCTAG	Mutation confirmation
E2F6–6R	AAGCGATTCTCCTGCCTCAG	
VPS45_F	TCCTGACCTCATGATCCACC	Mutation confirmation
VPS45_R	GCTGCCTCTGAAAACAATATTCC	
MRPS21_F	TGTCTAACCTCATTGCTTGCC	Mutation confirmation
MRPS21_R	TGGAGAGAAAACTGGATGAGG	
IFNB1_F	CAGGTAGTAGGCGACACTGT	Mutation confirmation
IFNB1_R	CATAGATGGTCAATGCGGCG	
DLG5_23F	GGAGGTAGCCAGAGTCTCAG	Mutation confirmation
DLG5_23R	AAGCGTGCAGATTGAGTGTC	
GUCY2C_23F	AGGGCTATGCTCATACTGTGT	Mutation confirmation
GUCY2C_23R	GGATGCATAGTGGGACCTCA	
CNN2_7F	CGCCTTGACCTCCCAAAC	Mutation confirmation
CNN2_7R	TGACACTCACAGACCCTTGG	
OAS3-FP	GAACTGTCCTGGGCCTGATCC	OAS3 real-time PCR
OAS3-RP	CATTCCCCAGGTCCCATGTGG	
ZIKA virus FP	AARTACACATACCARAACAAAGTGGT	Used for ZIKA virus detection
ZIKA virus RP	TCCRCTCCCYCTYTGGTCTTG	
HSV FP	CCGGAAACAACCCTACAACC	Used for HSV detection
HSV RP	TCGTGTATGGGGCCTTGG	

China) to monitor the mRNA synthesis. Thermal cycling conditions were identical for all primers and the two steps method was used. Each reaction was performed in triplicate, and the amplification products were examined by agarose gel electrophoresis and melting curve analysis. The relative gene expression level of OAS3 was calculated by normalizing to the reference genes. We divided the mRNA expression level of OAS3 in patients to that of the healthy controls, which was set as 1. Primers for reference and target genes are presented in Table 2. Three independent cDNA preparations were analyzed with three technical replicas each.

Construction of Vectors and Western Blotting

Plasmids encoding either wild-type (WT) or mutated-type (c.2299C>T: p.Arg767Cys) (MT) of OAS3 were constructed by commercial service provided by GeneCopoea (Guangzhou, China) (empty vector: pEZ-Lv242, Flag-tagged). Using lipotransfectamine 3000 (Invitrogen), those plasmids were transfected into HEK293T cells, which were cultured at 37 °C in a 5% CO2 incubator for another 24 hours in Dulbecco's modified Eagle's medium supplemented with 10% fetal bovine serum and 1% Pen/Strep. Cells were then lysed with 1× RIPA buffer supplemented with complete protease inhibitor (Roche, Shanghai, China) and the total proteins were quantified with BCA protein quantification kit. Western blotting was performed to analyze the protein expression level of WT and MT of OAS3 with anti-OAS3 antibody (Abcam, Cambridge, MA, USA). Glyceraldehyde-3-phosphate dehydrogenase (GAPDH) was used as a loading control.

Detection of Herpes Simplex Virus (HSV) and ZIKA Virus

To investigate HSV and ZIKA virus within this family, we extracted genomic DNA or total RNA from the blood samples which were stored in a –80°C fridge. HSV was detected by PCR with the genomic DNAs (50 ng) as a template using primer set listed in Table 2. The cDNA was synthesized from total RNA and used for the PCR analysis for ZIKA virus with primer set listed in Table 2. The PCR conditions were as follows: initial activation at 94°C for 5 minutes, then 30 amplification cycles of denaturation at 95°C for 15 seconds, followed by annealing and extension at 58°C for 30 seconds.

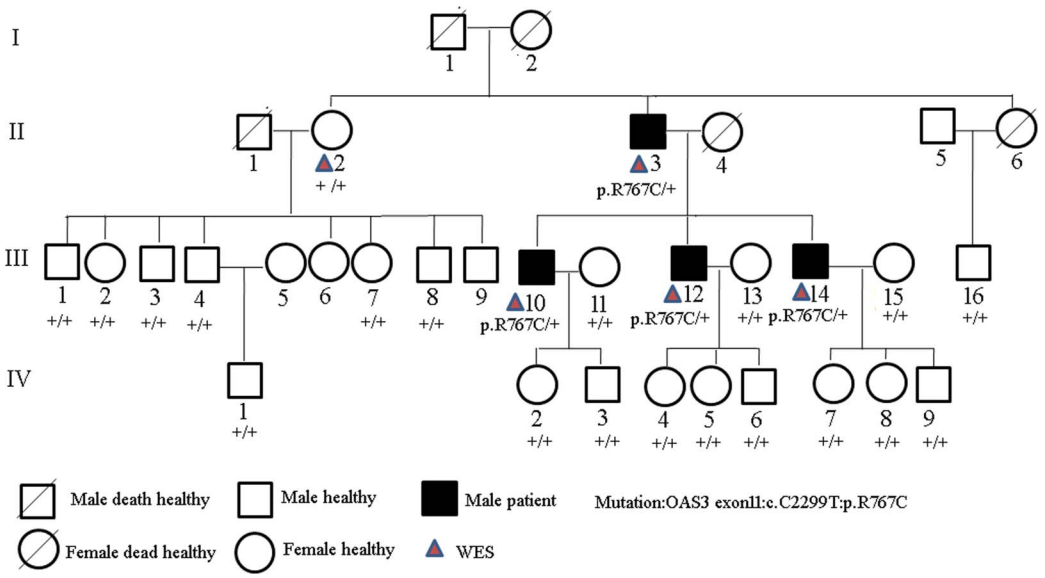

FIGURE 1. Pedigree of a Chinese JOAG family. A heterozygous missense mutation exon 11: c.2299C>T: p.Arg767Cys in the OAS3 gene was identified in subjects II:3, III:10, III:12, and III:14.

RESULTS

We recruited a two-generation glaucoma family containing four patients and 20 unaffected controls (Fig. 1). Based on the diagnosis ages (II:3, 40 years old; III:10, 38 years old; III:12, 35 years old; III:13, 31 years old) (Table 1), we considered this family as a JOAG family. All the patients showed high IOP (Table 1), therefore, IOP might be a risk factor to the development of JOAG. Patient II:3 has already been blind before he visited our hospital, and high IOP for his both eyes lasted for several years. Patient III:10 also showed high IOP; however, this patient could maintain a normal level of IOP for a long period (several years) after taking the anti-IOP medicine for several times. Both patients III:12 and III:14 showed progressive deterioration to vision with a concentrically constricted field (Figs. 2A, 2B). The visual acuity for all the patients was very low or blind (Table 1). Ophthalmologic examinations for the unaffected members within this family were also performed and the clinic features are listed in Table 1. Unaffected members IV:2, IV:3, and IV:5, who were still young at their first visit to our hospital (2008) for clinic check. Those three members did ophthalmologic examinations again at 2018 in our hospital and the results showed that they were still normal in both visual field and optical coherence tomography test (Supplementary Data S2; Table 1).We hence considered those individuals as unaffected controls for the next cosegregation analysis.

Here, WES coupled with Sanger sequencing was performed to identify the disease-causing mutations of this family. Blood samples from patients or unaffected controls were used to extract the genomic DNAs, which were sent for WES using commercially available service. Based on WES data, we noticed three variants in MYOC, a validated POAG-causing gene. Whereas all those variants located at the intronic region; we thus excluded those variants. Through step-wise filtering, we finally found 17 variants that present in all patients but are absent in the unaffected controls (Table 3). Of those, 14 were missense variants, one stop-gain variant, and two frameshift variants (Table 4). All 17 variants were predicted to be deleterious via SIFT, Polyphen2, CADD, and MT (Table 4). Based on the frequency assessment of ExAC ALL/EAS, we found that all the candidate variants were rare variants (less than 0.001).

PCR-based Sanger sequencing was performed to validate the above identified variants. The variant exon 6: c.C695A:p.P232H in CNN2 could not be confirmed in the subsequent Sanger sequencing and the remaining variants were validated and are listed in Table 4. All validated variants were present in all four patients (II: 3, III:10, III:12, III:14), but absent in the unaffected control (II:2) (Table 5). Applying Sanger sequencing, we performed the cosegregation analysis. Those variants (in ACIN1, OR6C75, SMARCC2, and IFNB1) occurring in unaffected family members (III:11, III:13, and III:15) were first excluded (Table 5). The remaining variants except the variant in OAS3 also could be excluded for being present in other unaffected controls, although some of unaffected members are still young; therefore, they should not be considered as a disease-causing variant (Table 5). To acquire more precise clinic data, ophthalmic examinations to the unaffected members IV:2 (27 years old) and IV:3 (25 years old) in 2018 were performed again, and the results showed that the eyes for both members were still unaffected. These results further supported that variant exon 11: c.2299C>T: p.Arg767Cys in OAS3 gene was a glaucoma-causing gene in this family (Table 4).To investigate whether this variant occurred in other POAG patients, we screened more than 200 unrelated POAG patients. A unrelated POAG patient carried the same OAS3 mutation (Supplementary Data S1). This patient also has high IOP and severe vision loss, although the onset age was older than 40 years (Supplementary Data S4). Moreover, after taking the anti-IOP medicine for several times, he also has maintained a normal level of IOP for a long time. At the same time, we detected other potential mutations in all exon of OAS3 gene within this family; we did not find other deleterious mutations (data not shown).

Through multiple protein sequences, alignment selected from several species, we found that amino acid residue ($Arg767^{th}$) was highly conservative in all OAS3 orthologs in various species (Fig. 3A), suggesting that residue (Arg767) plays important roles in maintaining the functions or structure of the OAS3 protein. To investigate the expression pattern of OAS3 in eye tissue, we retrieved its expression data from the GenePaint database. The section from E14.5 mouse embryo hybridized with RNA probe specific to OAS3 produces a strong signal band at the retina region, suggesting a high level of

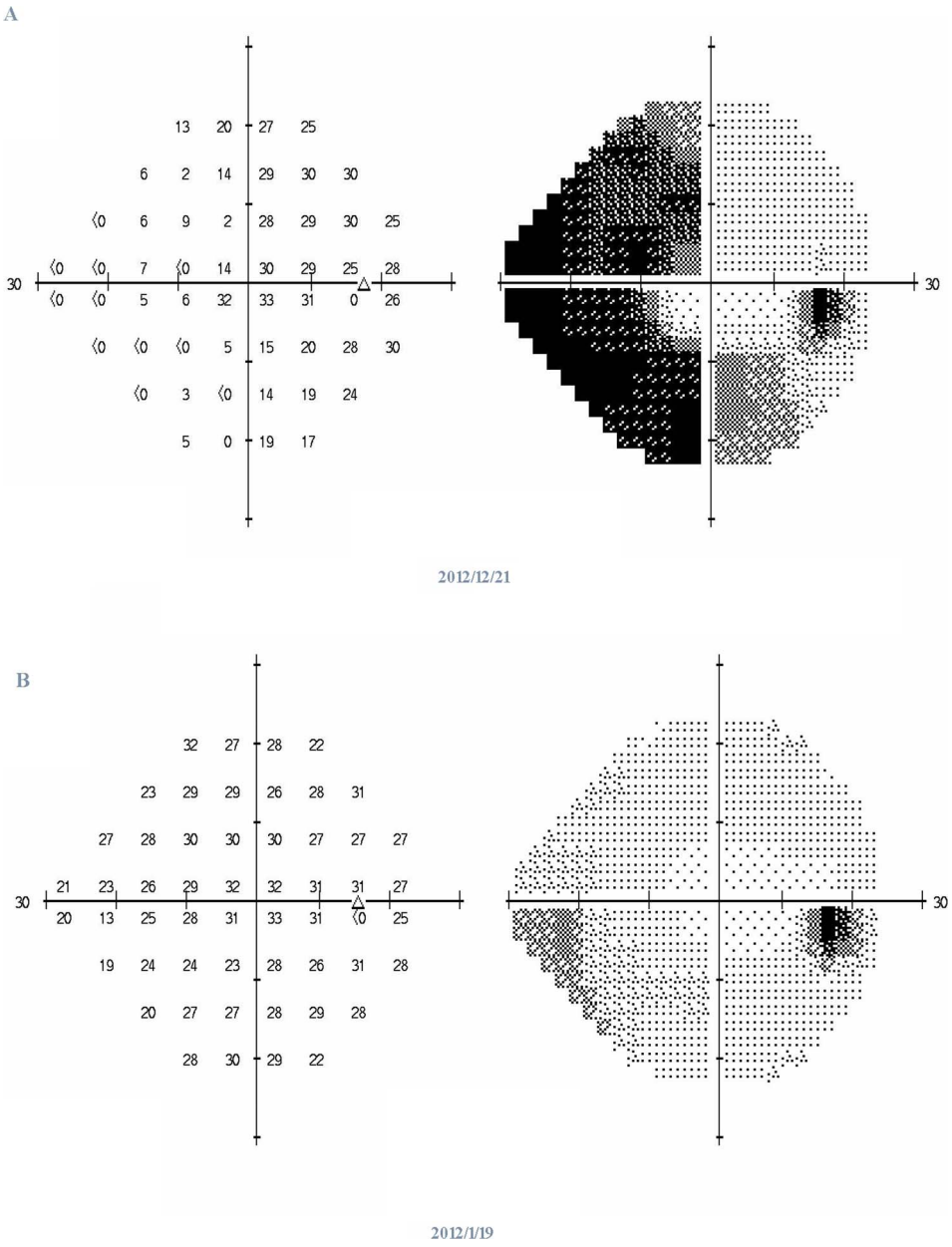

Figure 2. Visual field check for the proband showed a progressive loss of visual field. (**A**) represents visual field check on December 21, 2012; (**B**) represents visual field check in on January 19, 2012.

Table 3. Filtering Strategy for WES

Filter Steps	Samples				
	II2	II3	III10	III12	III14
Exonic variants, splicing site variants	24440	24752	24453	24569	24775
Nonsynonymous variants, stop-gain variants, stoploss variants, and coding indels	11538	11668	11551	11597	11455
Minor allele frequency <1% or absent	1527	1493	1481	1051	1481
Heterozygous variants shared by the four affected exomes			248		
Not found in unaffected exome			45		
Predicted to be deleterious			22		
Not found in house controls			17		

The filtering criteria are given on the left side of the workflow. The number of variants that remain after each filtering step is shown in the workflow. The 17 candidate variants were obtained as shown in Table 3.

Table 4. Candidate Variants Screened From the WES

Gene Name	ExonicFunc	AAChange.refGene	1000g 2015aug_all	ExAC ALL	ExAC EAS	Snp138	SIFT	Polyphen2_ HDIV	Mutation Taster	CADD	III:12	III:14	III:10	II:3	II:2
VPS45	Nonsynonymous SNV	NM_001279353:exon4:c.G193A:p.V65M	–	9.06E-05	0.0013	–	T	D	D	18.79	0/1:255,0,255	0/1:255,0,255	0/1:255,0,255	0/1:255,0,255	0/0:0,255,255
MRPS21	Nonsynonymous SNV	NM_018997:exon2:c.G185A:p.R62Q	–	0.0001	0.0014	–	T	P	D	24.9	0/1:255,0,255	0/1:255,0,255	0/1:255,0,255	0/1:255,0,255	0/0:0,181,255
MRPL9	Nonsynonymous SNV	NM_001300733:exon3:c.C408G:p.N136K	0.000599	0.0004	0.0058	rs200876352	D	D	D	17.5	0/1:201,0,255	0/1:248,0,255	0/1:255,0,193	0/1:255,0,255	0/0:0,93,255
KIDINS220	Nonsynonymous SNV	NM_020738:exon13:c.C1375T:p.P459S	0.0002	4.14E-05	0.0006	rs192644124	D	D	D	28.6	0/1:255,0,255	0/1:255,0,255	0/1:255,0,255	0/1:255,0,255	0/0:0,255,255
E2F6	Nonsynonymous SNV	NM_001278278:exon3:c.C202G:p.L68V	–	–	–	–	D	D	D	15.01	0/1:126,0,154	0/1:224,0,178	0/1:109,0,156	0/1:133,0,182	0/0:0,66,255
IFNB1	Nonsynonymous SNV	NM_002176:exon1:c.C102A:p.S34R	0.001797	0.0003	0.0037	rs139262191	T	D	N	16.56	0/1:255,0,255	0/1:255,0,255	0/1:255,0,255	0/1:255,0,255	0/0:0,160,255
DLG5	Nonsynonymous SNV	NM_004747:exon25:c.G4762T:p.A1588S	0.000998	0.0002	0.003	–	T	P	N	21.5	0/1:255,0,255	0/1:255,0,255	0/1:255,0,255	0/1:255,0,255	0/0:0,208,255
KLRD1	Nonsynonymous SNV	NM_007334:exon3:c.C112T:p.R38W	0.000599	0.0001	0.0021	rs189623484	D	D	N	11.46	0/1:255,0,255	0/1:255,0,255	0/1:255,0,255	0/1:255,0,255	0/0:0,253,255
GUCY2C	Nonsynonymous SNV	NM_004963:exon23:c.G2663A:p.R888Q	0.000998	0.0002	0.0024	rs373549158	T	P	D	23.3	0/1:255,0,255	0/1:125,0,254	0/1:203,0,255	0/1:228,0,255	0/0:0,48,255
OR6C75	Frameshift deletion	NM_001005497:exon1:c.305delT:p.F102fs	–	–	–	–	–	–	–	–	0/1:46,0,52	0/1:55,0,48	0/1:50,0,43	0/1:53,0,25	0/0:0,217,97
SMARCC2	Nonsynonymous SNV	NM_003075:exon22:c.A2260T:p.S754C	0.001398	0.0002	0.003	rs111975931	D	D	D	13.26	0/1:180,0,255	0/1:255,0,255	0/1:255,0,255	0/1:208,0,255	0/0:0,120,255
SHMT2	Nonsynonymous SNV	NM_001166356:exon4:c.C361T:p.R121C,	0.001198	0.0003	0.0035	rs375584473	D	D	D	25.8	0/1:255,0,255	0/1:255,0,255	0/1:255,0,255	0/1:255,0,255	0/0:0,255,255
OAS3	Nonsynonymous SNV	NM_006187:exon11:c.C2299T:p.R767C	0.0002	0.0004	0.0055	rs187467512	D	D	N	15.79	0/1:255,0,255	0/1:255,0,255	0/1:250,0,255	0/1:255,0,255	0/0:0,111,255
ACIN1	Stop-gain	NM_001164815:exon5:c.1808_1809insACGTTA: p.S603delinsSRX,	–	–	–	–	–	–	–	–	0/1:255,0,255	0/1:255,0,255	0/1:255,0,255	0/1:255,0,255	0/0:0,205,255
RIPK3	Frameshift insertion	NM_006871:exon10:c.1533dupT:p.G511fs	–	–	–	–	–	–	–	–	0/1:133,0,104	0/1:169,0,86	0/1:171,0,145	0/1:122,0,137	0/0:0,30,151
KIF26A	Nonsynonymous SNV	NM_015656:exon4:c.G757A:p.V253M	0.000399	0.0001	0.0004	rs371230681	D	D	N	12.22	0/1:255,0,255	0/1:255,0,255	0/1:255,0,255	0/1:255,0,255	0/0:0,217,255
CNN2	Nonsynonymous SNV	NM_201277:exon6:c.C695A:p.P232H	–	8.57E-05	0	rs75676484	D	D	D	22.6	0/1:102,0,255	0/1:93,0,167	0/1:70,0,255	0/1:9,0,255	0/0:0,18,255

AAChange, amino acid change; CADD, Combined Annotation Dependent Depletion; ExAC ALL, all variants in The Exome Aggregation Consortium (ExAC); ExAC EAS, Variants in east Asian population in The Exome Aggregation Consortium; ExonicFunc, exon function; 1000g2015aug_all, 1000 genomes project, 2015, all site; SNV, single nuclear variation; III:12 III:14 III:10 II:3 are patients, II:2, healthy control. 0/1: Variant represents in one allele; 0/0: represent no mutation in both alleles.

Table 5. Cosegregation Analysis Within Family

Gene and Variants	III:12	III:14	III:10	II:3	III:1	II:2	III:7	III:3	III:2	III:4	III:8	IV:1	IV:2	IV:3	IV:4	IV:5	IV:6	IV:7	IV:8	III: 11	III: 13	III: 15
KIF26A.exon4:c.G757A:p.V253M	0/1	0/1	0/1	0/1	0/0	0/0	0/0	0/0	0/0	0/0	0/0	0/0	0/0	0/1	0/0	0/0	0/0	0/0	0/1	0/0	0/0	0/0
RIPK3:exon10:c.1533dupT:p.G511fs	0/1	0/1	0/1	0/1	0/0	0/0	0/0	0/0	0/0	0/0	0/0	0/0	0/1	0/1	0/0	0/0	0/1	0/1	0/1	0/0	0/0	0/0
MRPL9:exon3:c.C408G:p.N136K	0/1	0/1	0/1	0/1	0/0	0/0	0/0	0/0	0/0	0/0	0/0	0/0	0/0	0/0	0/0	0/1	0/0	0/0	0/1	0/0	0/0	0/0
KLRD1:exon3:c.C112T:p.R38W	0/1	0/1	0/1	0/1	0/0	0/0	0/0	0/0	0/0	0/0	0/0	0/0	0/1	0/0	0/0	0/0	0/1	0/0	0/0	0/0	0/0	0/0
KIDINS220:exon13:c.C1375T:p.P459S	0/1	0/1	0/1	0/1	0/0	0/0	0/0	0/0	0/0	0/0	0/0	0/0	0/1	0/1	0/0	0/1	0/0	0/0	0/0	0/0	0/0	0/0
SMARCC2:exon22:c.A2260T:p.S754C	0/1	0/1	0/1	0/1	0/0	0/0	0/0	0/0	0/0	0/0	0/0	0/0	0/0	0/0	0/1	0/0	0/1	0/0	0/0	0/0	0/1	0/0
ACIN1:exon5:c.1808_1809insACGTTA:p.S603delinsSRX	0/1	0/1	0/1	0/1	0/0	0/0	0/1	0/0	0/1	0/1	0/1	0/1	0/0	0/0	0/1	0/1	0/1	0/0	0/1	0/1	0/1	0/1
OAS3:exon11:c.C2299T:p.R767C	**0/1**	**0/1**	**0/1**	**0/1**	**0/0**	**0/0**	**0/0**	**0/0**	**0/0**	**0/0**	**0/0**	**0/0**	**0/0**	**0/0**	**0/0**	**0/0**	**0/0**	**0/0**	**0/0**	**0/0**	**0/0**	**0/0**
SHMT2:exon4:c.C361T:p.R121C	0/1	0/1	0/1	0/1	0/0	0/0	0/0	0/0	0/0	0/0	0/0	0/0	0/0	0/0	0/0	0/0	0/1	0/0	0/0	0/0	0/0	0/0
OR6C75:exon1:c.305delT:p.F102fs	0/1	0/1	0/1	0/1	0/0	0/0	0/0	0/0	0/0	0/0	0/0	0/0	0/1	0/1	0/1	0/1	0/0	0/1	0/1	0/1	0/0	0/0
E2F6:NM_001278278:exon3:c.C202G:p.L68V	0/1	0/1	0/1	0/1	0/0	0/0	0/0	0/0	0/0	0/0	0/0	0/0	0/1	0/1	0/0	0/1	0/0	0/0	0/0	0/0	0/0	0/0
VPS45:NM_007259:exon4:c.G301A:p.V101M	0/1	0/1	0/1	0/1	0/0	0/1	0/0	0/0	0/0	0/0	0/0	0/0	0/0	0/0	0/0	0/1	0/0	0/0	0/1	0/0	0/0	0/0
MRPS21:NM_018997:exon2:c.G185A:p.R62Q	0/1	0/1	0/1	0/1	0/0	0/0	0/0	0/1	0/0	0/0	0/0	0/0	0/0	0/0	0/0	0/0	0/0	0/0	0/1	0/0	0/0	0/0
IFNB1:NM_002176:exon1:c.C102A:p.S34R	0/1	0/1	0/1	0/1	0/0	0/0	0/0	0/0	0/0	0/0	0/0	0/0	0/0	0/0	0/1	0/1	0/0	0/0	0/0	0/1	0/0	0/0
DLG5:NM_004747:exon25:c.G4762T:p.A1588S	0/1	0/1	0/1	0/1	0/0	0/0	0/0	0/0	0/0	0/0	0/0	0/0	0/1	0/1	0/1	0/0	0/0	0/0	0/0	0/0	0/0	0/0
GUCY2C:NM_004963:exon23:c.G2663A:p.R888Q	0/1	0/1	0/1	0/1	0/0	0/0	0/0	0/0	0/0	0/0	0/0	0/0	0/1	0/0	0/0	0/0	0/1	0/0	0/0	0/0	0/0	0/0

The values in bold indicate the screened OAS3 variant present in patients, but not in healthy controls.

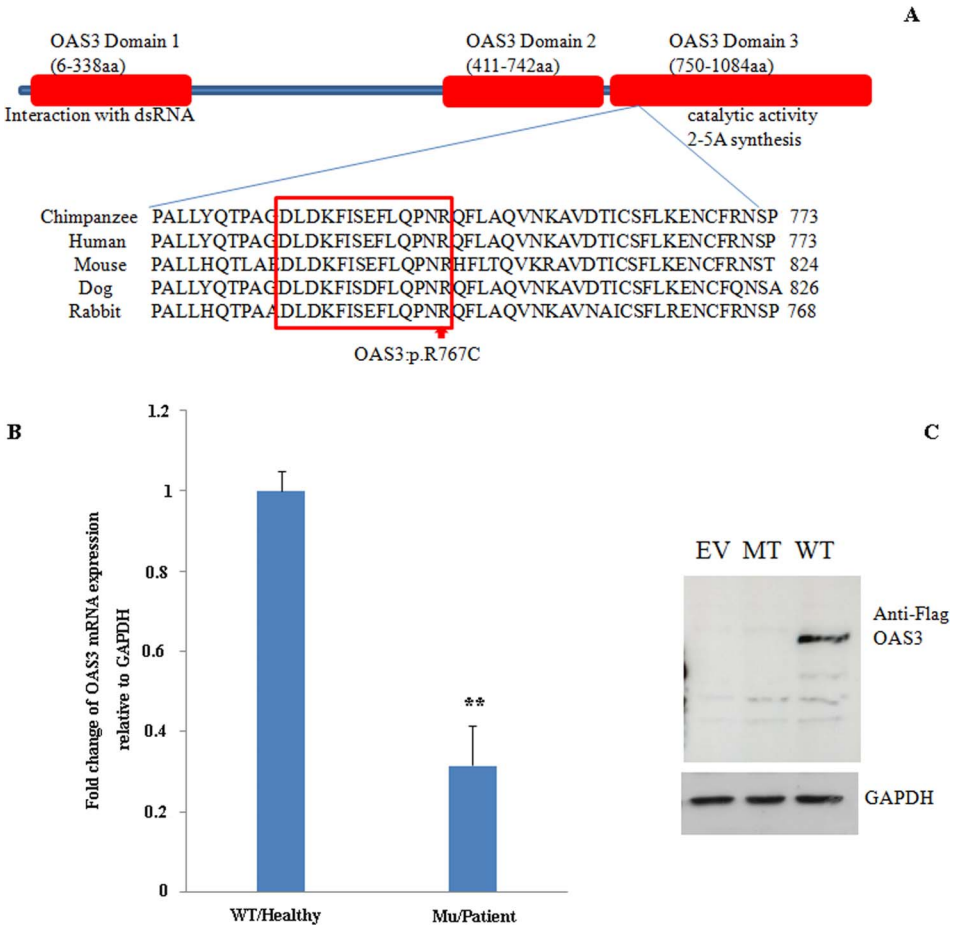

FIGURE 3. Location and conservation of mutated amino acid residue, and the expression of OAS3. (**A**) Mutated amino acid residue (R) locates at the OAS3 domain 3. Multiple sequence alignment of the region of the *OAS3* protein surrounding the mutation in various species. The Arg residue (indicated with a *red arrow*) is highly conserved among all species analyzed (chimpanzee, human, mouse, dog, and rabbit). (**B**) qPCR analysis for the mRNA expression of OAS3 in blood from patients and healthy controls within this family. Three independent experiments were performed. *Error bar* shows SD (average expression fold change ± SD), Student's *t*-test was used for the *P* value analysis. $^{**}P < 0.01$. (**C**) Plasmids encoding either WT OAS3 or a version of MT OAS3 were transfected into HEK293T cells and the protein expression of OAS3 was then validated by Western blot with anti-OAS3 antibody. GAPDH was used as a loading control. The experiments were repeated three times. EV, empty vector.

mRNA transcription (Supplementary Fig. S1). Through extracting the total RNAs from the peripheral blood of family members (including patients and healthy controls), we further compared the mRNA expression of OAS3 in patients and healthy controls via qPCR. The results showed that the mRNA expression level of OAS3 significantly decreased in patients compared with that of the healthy controls (Fig. 3B). Moreover, the protein expression of either recombinant WT OAS3 or a version harboring the mutation (MT) OAS3 protein in HEK293T was investigated by Western blot. The recombinant WT OAS3 protein showed a strong blotting band; however, recombinant MT OAS3 band almost disappeared, probed by the anti-OAS3 antibody (Fig. 3C).We also found HSV DNA from blood genomic DNA and gene expression of ZIKA virus in the blood RNA of patients and some of the unaffected individuals (Supplementary Fig. S2) Taking above data together, we argued that mutation in OAS3 led to mRNA degradation and resulted in a low level of protein expression.

DISCUSSION

As a risk factor of permanent blindness, approximately 10% of patients with glaucoma become blind despite improvement of clinical treatment.[13] Here we found a disease-causing variant in *OAS3* from a Chinese JOAG family. During the cosegregation analysis, we considered two family members IV:2 and IV:3 as healthy controls. However, their current ages are still younger than 35 years, the average onset age of this family. Hence, we cannot completely exclude the possibility that these two members will develop POAG in the future. However, to confirm the variant that we identified was the bona fide disease-causing mutation for this family, we will perform a follow-up survey of 10 years to this family.

Accumulating evidence supports that high IOP is not the only risk factor for the development of POAG. For instance, patients with normal-tension glaucoma also show retinal ganglion cell (RGC) loss; on the other hand, patients with high IOP contain healthy RGCs.[13,14] Inflammation was frequently observed in ocular tissues of patients with glaucoma, such as interleukin-20,[15] neuroinflammation,[16] and other cytokines.[17] Prostaglandins are small proinflammatory molecules derived from arachidonic acid and their analogues are frequently used to treat glaucoma.[18] Virus infections such as ZIKA and cytomegalovirus can damage ocular tissues via activating inflammation-associated pathways.[19,20] OAS3 can synthesize 2′, 5′-oligoadenylates (2–5A) from ATP on binding to double-stranded (ds)RNA and is specialized for binding long dsRNA.[21] OAS3 activates RNase L endonuclease in response to

exogenous RNA from either virus or bacteria,[21–24] suggesting that the OAS/RNaseL pathway is a major antiviral defense mechanism.[21–25] Recent research revealed that OAS3 could activate RNase L and inhibited ZIKA virus replication.[26] Therefore, OAS3 mutation enhances the host's susceptibility to viral or bacterial infection, which in turn, activates their inflammation. This was further confirmed by the virus genomic DNA or RNAs detected from the blood samples of family members including patients and healthy controls (Supplementary Fig. S2).Therefore, the pathological development of glaucoma in this family might be induced by infection. Infection might be more severe in patients harboring the OAS3 mutation than that in healthy controls with a normal OAS3 gene, leading to higher inflammation and finally promoting the development of glaucoma.

Taken together, OAS3 mutation c.2299C>T: p.Arg767Cys causes the development of JOAG in a Chinese family. This mutation led to a deleterious effect to its mRNA and protein expression.

Acknowledgments

Supported by the National Natural Science Foundation of China (grant no. 81470636) and the "Talent Project" in sailing plan of Guangdong Province.

Disclosure: **X. Xiao**, None; **C. Huang**, None; **Y. Cao**, None; **S. Chen**, None; **Y. Xu**, None; **H. Chen**, None; **C. Pang**, None; **M. Zhang**, None

References

1. Alward WLM, Van der Heide C, Khanna CL, et al. Myocilin mutation in patients with normal-tension glaucoma. *JAMA Ophthalmol*. 2019;137:559–563.
2. Kwo HS, Johnson TV, Joe MK, et al. Myocillin mediates myelination in the peripheral nervous system through ErbB2/3 signaling. *J Biol Chem*. 2013;288:26357–26371.
3. Ge T, Chen CY, Neale BM, et al. Phenome-wide heritability analysis of the UK Biobank. *PLoS Genet*. 2017;13:e1006711.
4. Wiggs JL, Pasquale LR. Genetics of glaucoma. *Hum Mol Genet*. 2017;26:R21–R27.
5. Wang R, Wiggs JL. Common and rare genetic risk factors for glaucoma. *Cold Spring Harb Perspect Med* 2014;4:a017244
6. MacGregor S, Ong JS, An J, et al. Genome-wide association study of intraocular pressure uncovers new pathways to glaucoma. *Nat Genet*. 2018;50:1067–1071.
7. Shiga Y, Akiyama M, Nishiguchi KM, et al. Genome-wide association study identifies seven novel susceptibility loci for primary open-angle glaucoma. *Hum Mol Genet*. 2018;27:1486–1496.
8. Springerlkamp H, Iglesias AI, Cuellar-Partida G, et al. ARHGEF12 influences the risk of glaucoma by increasing intraocular pressure. *Hum Mol Genet*. 2015;24:2689–2699.
9. Gong B, Zhang H, Huang L, et al. Mutant RAMP2 causes primary open-angle glaucoma via the CRLR-cAMP axis [published online ahead of print April 19, 2019]. *Genet Med*. doi:10.1038/s41436-019-0507-0.
10. Choquet H, Paylakhi S, Kneeland SC, et al. A multiethnic genome-wide association study of primary open-angle glaucoma identifies novel risk loci. *Nat Commun*. 2018;9:2278.
11. Xiao X, Cao Y, Zhang Z, et al. Novel mutations in PRPF31 causing retinitis pigmentosa identified using whole-exome sequencing. *Invest Ophthalmol Vis Sci*. 2017;58:6342–6350.
12. Geng X, Irvin MR, Hidalgo B, et al. An exome-wide sequencing study of the goldn cohor reveals novel associations of coding variants and fasting plasma lipids. *Front Genet*. 2019,10:158
13. Moroi SE, Reed DM, Sanders DS, et al. Precision medicine to prevent glaucoma-related blindness. *Curr Opin Ophthalmol*. 2019;30:187–198.
14. Krishnan A, Fei F, Jones A, et al. Overexpression of soluble fas ligand following adeno-associated virus gene therapy prevents retinal ganglion cell death in chronic and acute murine models of glaucoma. *J Immunol*. 2016;197:4626–4638.
15. Wirtz MK, Keller KE. The role of the IL-20 subfamily in glaucoma. *Mediators Inflamm*. 2016;2016:4083735.
16. Williams PA, Marsh-Armstrong N, Howell GR. Neuroinflammation in glaucoma: a new opportunity. *Exp Eye Res*. 2017;157:20–27.
17. Ten Berge JC, Fazil Z, van den Born I, et al. Intraocular cytokine profile and autoimmune reactions in retinitis pigmentosa, age-related macular degeneration, glaucoma and contaract. *Acta Ophthalmol*. 2019,97:185–192.
18. Doucette LP, Walter MA. Prostaglandins in the eye: function, expression, and roles in glaucoma. *Ophthalmic Genet*. 2017;38:108–116.
19. Singh PK, Kasetti RB, Zode GS, et al. Zika virus infects trabecular meshwork and causes trabeculitis and glaucomatous pathology in mouse eyes. *mSphere*. 2019;4:e00173–19.
20. Choi JA, Kim JE, Noh SJ, et al. Enhanced cytomegalovirus infection in human trabecular meshwork cells and its implication in glaucoma pathogenesis. *Sci Rep*. 2017;7:43349.
21. Lee WB, Choi WY, Lee DH, et al. OAS1 and OAS3 negatively regulate the expression of chemokines and interferon-responsive genes in human macrophages. *BMB Rep*. 2019;52:133–138.
22. Nogimori T, Nishiura K, Kawashima S, et al. Dom34 mediates targeting of exogenous RNA in the antiviral OAS/RNase L pathway. *Nucleic Acids Res*. 2019;47:432–449.
23. Silverman RH. Viral encounters with 2′,5′-oligoadenylate synthetase and RNase L during the interferon antiviral response. *J Virol*. 2007;81:12720–12729.
24. Ireland DD, Stohlman SA, Hinton DR, et al. RNase L mediated protection from virus induced demyelination. *PLoS Pathog*. 2009;5:e1000602.
25. Li YZ, Banerjee SV, Wang YY, et al. Activation of RNase L is dependent on OAS3 expression during infection with diverse human viruses. *PNAS*. 2016;113:2241–2246.
26. Whelan JN, Li Y, Silverman RH, Weiss SR. Zika virus production is resistant to RNaseL antiviral activity. *J Virol*. 2019;93:e00313–19.